Repairing brickwork panels using titanium rods embedded in the mortar joints

Marco Corradi[1,2]*, Giulio Castori[2] and Antonio Borri[2]

[1]Northumbria University, Department of Mechanical and Construction Engineering
Wynne Jones Building, Newcastle upon Tyne, NE1 8ST, United Kingdom

[2]University of Perugia, Department of Engineering,
Via Duranti 93, 06125 Perugia, Italy

ORCID 0000-0003-3872-3303 (Corradi)
ORCID 0000-0002-1541-0673 (Castori)
ORCID 0000-0002-5872-4947 (Borri)

* corresponding author
email marco.corradi@northumbria.ac.uk
Tel. +44 (0) 191 215 3741, Fax. +44 (0) 191 215 3725

KEYWORDS: Historic masonry, micro-modeling, titanium, retrofitting methods, shear strength.

ABSTRACT

This paper investigates repairing brickwork masonry walls using smooth titanium rods. Firstly, numerical analyses were carried out following a detailed micro-modelling strategy and then an experimental research program was undertaken in the laboratory. Solid clay brick specimens were initially tested, without strengthening, and subsequently re-tested, after repair, using titanium rods. Rods were embedded into the horizontal joints using an epoxy paste or a cement mortar. A double-sided repair was considered. Shear tests were carried out on four brickwork panels, under diagonal loading. The mechanism by which the diagonal shear load was carried was analyzed, varying from the uncracked state, to the final, cracked state, for both control and repaired wall panels. The results demonstrate that it is partially possible to restore the panels' original in-plane shear capacity by embedding titanium rods into the horizontal bed joints using the epoxy paste. The experimental results were used to evaluate the effectiveness of the titanium repair, and recommendations are made to allow the test data to be used in the design procedure of cracked masonry structures. Unsatisfactory test results were recorded for panels repaired using a cement mortar.

1. INTRODUCTION

During the last two decades, new retrofitting methods of pre-existing historic masonry walls have been extensively used in Europe in construction because of the seismic hazard, or the need to comply with new safety restrictions or new building codes [1][2][3][4][5]. Several methods have been proposed and experimented both on-site and in the laboratory, and many of them demonstrated to be effective in increasing the in-plane capacity (shear strength) of wall panels.

Since the early 2000s, extensive research has been carried out to reinforce pre-existing masonry buildings or masonry members using externally epoxy-bonded FRP (Fiber Reinforced Polymers) materials [6][7][8][9][10]. In Civil Engineering, these materials are still regarded as innovative. FRPs have now become popular as a shear reinforcement of wall panels because they have high tensile strength, extraordinary strength-to-weight ratios and are effectively corrosion free. However, FRPs are costly and difficult to install due to the combined use of epoxies.

On opposite, traditional methods [grout injections, RC (Reinforced Concrete) jacketing] are typically cost-effective and easy to install compared with innovative methods [11][12][13][14]. Most of these methods can be applied quickly with a minimal intrusion and increment of mass, making them suitable for seismic reinforcement or repair.

FRP sheets and cloths can be easily applied, with minimal disruption to the structure and rapid completion. These composites are directly applied on the brick or stone surface of the un-plastered walls using an epoxy or polyester adhesive. Apart for the safety hazards of workers using these toxic adhesives, there are critical open issues in the use of FRPs: 1. the unsatisfactory long term behavior of composites, with significant reductions of the FRP mechanical properties during ageing, 2. the low glass transition temperature of the adhesives, with the risk of FRP deboning from masonry if exposed to hot summer temperatures, likely to occur in many southern Europe countries, 3. the low fire resistance of FRPs, 4. the difficulty to comply with the requirement of “reversiveness” (according to the ICOMOS principles for interventions of monuments and sites “Where possible, any measures adopted should be “reversible” so that they can be removed and replaced with more suitable measures when new knowledge is acquired. Where they are not completely reversible, interventions should not limit further interventions” [15]), 5. the impossibility to keep the fair faced aspect of the masonry when reinforced or repaired with FRP sheets or cloths.

It is true that not all the above are an issue: for example “reversiveness” is important only for listed monuments and heritage buildings, the need to keep the fair faced aspect of the masonry is not always required, mechanical degradation of FRPs is mitigated by their very high tensile strength, making it a managing problem. However, it can be concluded that prudence should be advised on the use of composite materials for shear reinforcement of masonry walls.

Joint repointing is another traditional method [16][17][18]. This is often used as a non-structural restoration technique for stone and brickwork walls. Repointing brick and stone work is the task of renewing the outer portion of the mortar joint with new mortar. Repointing provides a primary defence against water ingress; it holds the stones/bricks in place so they don’t move, increasing the overall stability and integrity of the walls and avoiding stress concentrations.

The structural characteristics of this method can be improved using a “deep repointing” [19]. When the thickness of the mortar joints is large enough to allow the repointing task up to a depth of 5-7 cm, this method acquires significant structural features. It has been demonstrated that it is possible to increase the masonry compressive strength by deep repointing.

However, limited research has been conducted on the shear resistance of wall panels strengthened by deep repointing. The application of a new lime mortar cannot overcome the intrinsic weak behavior of masonry in tension, as a result of the use of the mortar itself. In order to overcome this problem, the repointing mortar can be reinforced using a tensile-resistant material [20][21]: Valluzzi et al. proposed to use steel bars and experimental tests and numerical analyses demonstrated that it is possible to reduce cracking of brickwork masonry [22]. A similar method, based on the use of metal or composite cords has been proposed by Borri et al. [23][24]: this method, known as "Reticulatus", can be used to reinforce irregular stone masonry. The use of flexible materials (i.e. the cords) is well suited for non-straight (i.e. the mortar joints of irregular/rubble stone masonry) mortar joints, and tests results demonstrated that it is possible to highly increase the lateral load capacity and stiffness of historic walls.

Furthermore, there are several commercial products on the construction market for crack stitching. Twisted bars are used for crack stitching repairs and for stabilizing cracked masonry [25][26]: stainless steel bars are typically bonded into cut slots with a high-strength grout. However, there is little experimental evidence of the effectiveness of this repair method and more analysis is needed. The damage induced by cut slots should be better investigated, especially when used on single-wythe brickwork walls.

This paper is aimed at studying the effect of the use of titanium rods, embedded into the horizontal mortar joints, without cutting slots. Rods are only used to repair locally the shear cracks of a brickwork panel, and are of limited length (300-500 mm). This method would nevertheless repair and not reinforce the shear walls, and the overall objective is to restore the original pre-cracking lateral capacity of the walls. First results of this experimental investigation were presented at conference level to acquire feedback from the scientific community [27].

2. THE REINFORCEMENT METHOD

Evidence strongly suggests that the growing popularity and use of new retrofitting methods of historic masonry buildings have been responsible for a substantial reduction of fatalities and damage during natural disasters. Historic buildings are at risk of major damage during seismic events and flooding. Climate changes are also responsible for new natural hazards such as heavy rain falls.

This experimental work is focused on the shear behavior of brickwork wall panels. Tests were carried out in the laboratory using four wall panels. The basic idea is to repair cracked panels with titanium rods embedded, across a shear crack, inside the horizontal bed joints.

Among the advantages of this repair method, we can note that titanium rods can be easily applied and, if needed, removed, and the use of titanium guarantees an excellent long term also for outdoor applications or aggressive environments. This repair method is interesting when the fair faced aspect of the masonry must be conserved and it can be used in combination with other traditional retrofitting techniques, such as grout injections.

The aim is to restore the original (pre-damage) lateral capacity of cracked wall panels by sealing the cracks with new mortar and a tensile-resistant material (metal bars, composite cords, cables, wires, etc.). In this work, the use of high-strength titanium rods was investigated. This repair method is also interesting if compared with other retrofitting methods (FRP sheets or steel-wire RC coatings), that can be overly invasive or non-reversible and therefore unacceptable from the point of view of conservation.

The repair method is based on the use of materials not difficult to find on the construction market. Rods can be made of titanium or stainless steel. The cost of titanium has recently fallen sharply. The weight density of titanium is about (4400-4500 kg/m^3) half of carbon steel, and typical yield strengths range between 300 MPa (Titanium grade 2) and 800 MPa (Ti-6Al-4V) [28] [29]. This implies that smaller rods can be used to absorb high tensile loads, facilitating the installation of the rods into the horizontal mortar joints.

The repair procedure of a cracked wall panel using the method suggested here is carried out in the following steps:

a) Strip and repoint of the horizontal mortar joints in the area of the shear crack, for a depth of 2-3 cm using new high strength mortar; given the localized area of intervention, it is also possible to use small quantities of epoxy paste: this could improve the bonding between the titanium rods and the bricks, facilitating the stress transfer by shear between the materials;

b) Rods should be installed, across the crack, on both wall sides. For single wythe brickmasonry masonry, it could be possible to apply the rods only on one face.

c) Length and diameter of the titanium rods depend on the type of brickwork masonry and wall dimensions. 7 mm-diameter rods are typically more than enough to absorb very high tensile stresses. Rod's lengths highly depend on the type of new mortar/epoxy paste used for embedment. Longer rods are necessary when mortar is used, while shorter rods can be employed in combination with an epoxy paste.

d) In order to avoid stress concentration, it is suggested to install the rods in a large number of bed joints. In this experimental work rods were installed in every second joint. More analysis will be necessary to better define and fix this construction detail.

e) A final layer of new mortar is subsequently applied over the rods to completely fill the gap in the horizontal joint. Rods are made invisible, while the fair-faced aspect of the masonry is fully preserved.

3. STRENGTHENING OF MASONRY PANELS WITH TITANIUM RODS: NUMERICAL MODELLING

Based on this background, the strategy proposed to investigate the proposed repairing technique was formally similar to a step-by-step procedure based on the use of numerical investigations and experimental tests. In detail, numerical analyses were used as a preliminary approach aimed at investigating, at local level, the main mechanical aspects (e.g. the influence of the different type of matrix - cementitious or epoxy - in the stiffness and strength of shear stressed masonry, as well as the effect the reinforcement action of titanium rods) required for designing the following experimental procedure. Next, after checking the positive effect of the reinforcing rods in repairing the masonry panels, their macroscale structural behavior was evaluated through laboratory investigations.

3.1. Modelling strategy

The formulation of effective and accurate methods to investigate the in-plane behavior of masonry structures is a challenging task. Because of the non-isotropic structural response of masonry that stems from its composite nature, the development of efficient structural analyses often required two- or three-dimensional modelling strategies, i.e. more complex structural schemes in comparison with those traditionally adopted for steel or concrete framed constructions.

Among the different modeling approaches provided in the recent literature, the use of non-linear models implemented in sophisticated Finite Element (FE) formulations seems to be the most promising [28][29]. Different scale strategies of different complexity [30][32][32] are usually adopted to model block masonry using FE analysis (Figure 1): macro, simplified micro and detailed micro scales.

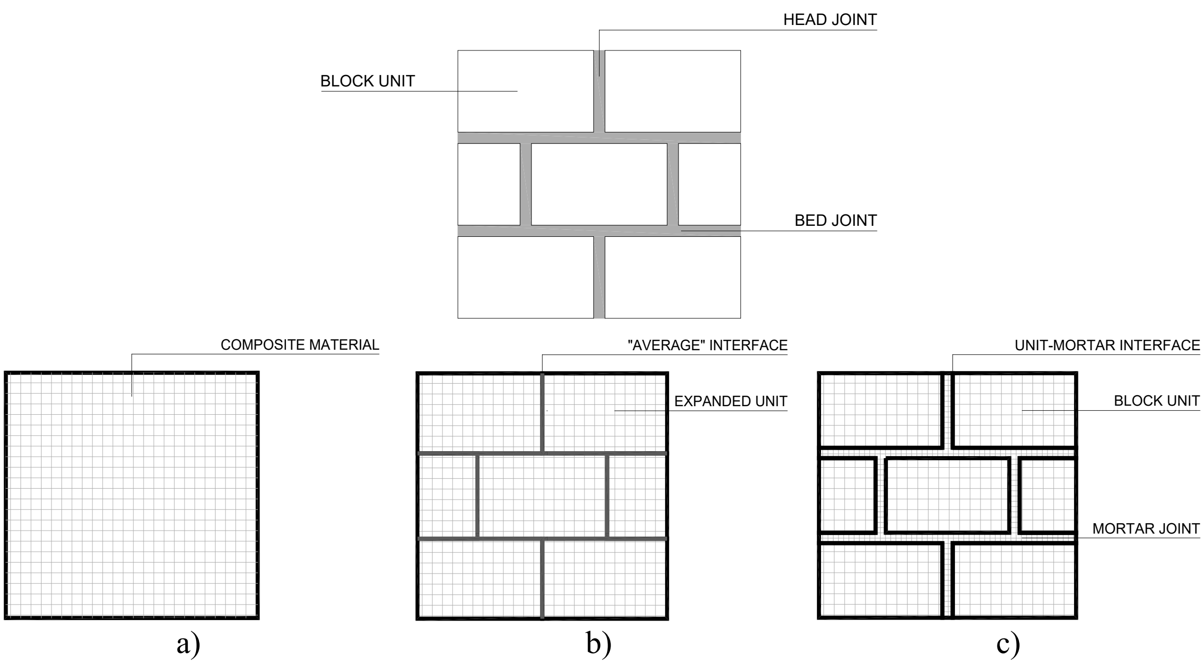

Figure 1: Modelling strategies of different complexity: a) Macro-modelling; b) Simplified micro-modelling; c) Detailed micro-modelling.

As far as macro-modelling strategy (Figure 1a), masonry constitutive laws are based on the assumption of a homogeneous material (either with non-isotropic or isotropic behavior), without distinguishing between mortar and block units (homogenized or smeared crack models). Due to the reduced computational effort, this type of approach is traditionally adopted in large and practice-oriented analyses, where a compromise between efficiency and accuracy is often needed. Nevertheless, a considerable limitation is its inability to model discontinuities (e.g. mortar to masonry interface) and hence local failure modes.

A satisfactory solution is the use of simplified micro-modelling procedures (Figure 1b), able to represent discontinuities in masonry. In this case, the computational strategy consists in lumping each mortar joint into an "average" interface (discontinuous element), while the block units are expanded (up to half of the joint thickness in the horizontal and vertical directions) to keep the wall geometry unchanged. By considering the interaction between mortar joints and block units, it is possible to obtain more accurate localized results; however, with this modelling approach, information about the actual crack pattern within the mortar is lost, since cracking can only occur at the interface and not in the masonry units.

Conversely, when a detailed micro-scale (Figure 1c) is used, the masonry is regarded as a heterogeneous material, made of mortar joints and block units joined through unit-mortar interfaces, which usually represent a potential crack (or slip) plane due to the coupling between different materials. To this end, all masonry components are modelled in detail by applying, separately, different elastic (and optionally inelastic) properties for each constituent. Therefore, despite large time and memory requirements, this approach enables a comprehensive analysis of the masonry material with a more realistic prediction of its shear behavior and local damage pattern.

With the aim at investigating the effect of the proposed repair method, numerical analyses were carried out, using a commercial FE modelling code, following a detailed micro-modelling strategy. The proposed FE analyses were based on a detailed micro-modelling approach, aimed at capturing the failure mechanisms (i.e. at monitoring the damaging process inside the mortar joints) as well as the masonry quasi-brittle behavior (i.e. cracking rather than a plastic yield) of masonry.

According to their capability of updating the geometric stiffness matrix at each integration by following the cracking during load application, a series of three-dimensional FE models was therefore developed to account for material non-linear response. To simplify the analysis (by reducing as much as possible the computational effort) displacement-controlled analyses were carried out. This was done by considering only the periodic basic cell extracted from the central part of the brickwork wall in Flemish bond. To this end, the periodically repeating arrangement was discretized by dividing the basic cell into fifty-nine cuboid sub-cells (forty-six brick units, two bed and eleven head joints) with different properties (Figure 2).

This approach, together with the assumption of a non-isotropic and heterogeneous material in which rigid rotations of brick units (much stiffer than mortar joints) and deformations of mortar joints can be induced, is similar to the formulation proposed by Mann and Müller [33]. Under these hypotheses, assuming a macroscopically homogeneous shear state, equilibrium can be attained only by normal stresses ($\pm\alpha\tau$) produced by shear stresses ($\pm\tau$) leading to a non-uniform distribution of the compressive stresses along the mortar joints (Figure 3).

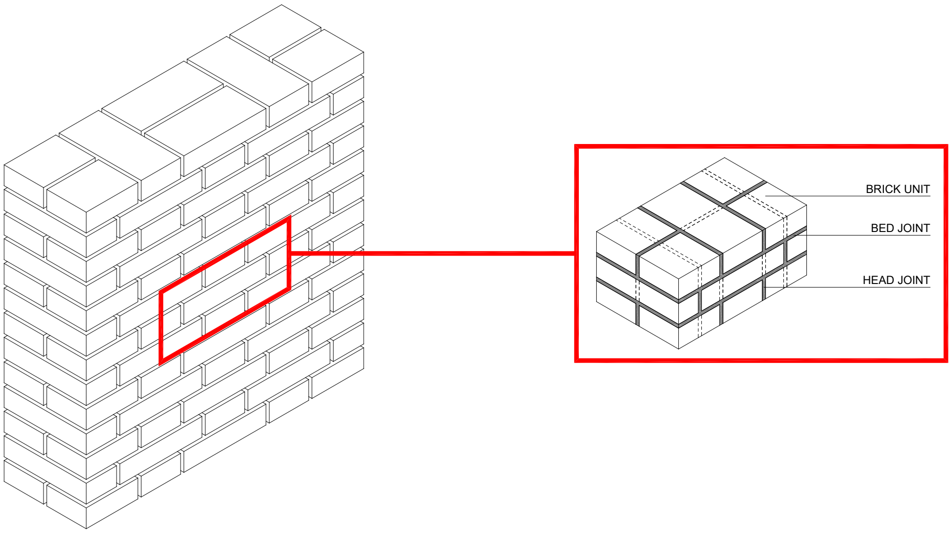

Figure 2: Discretization and component designation of the periodic basic cell extracted from the central part of a masonry wall (Flemish bond wall).

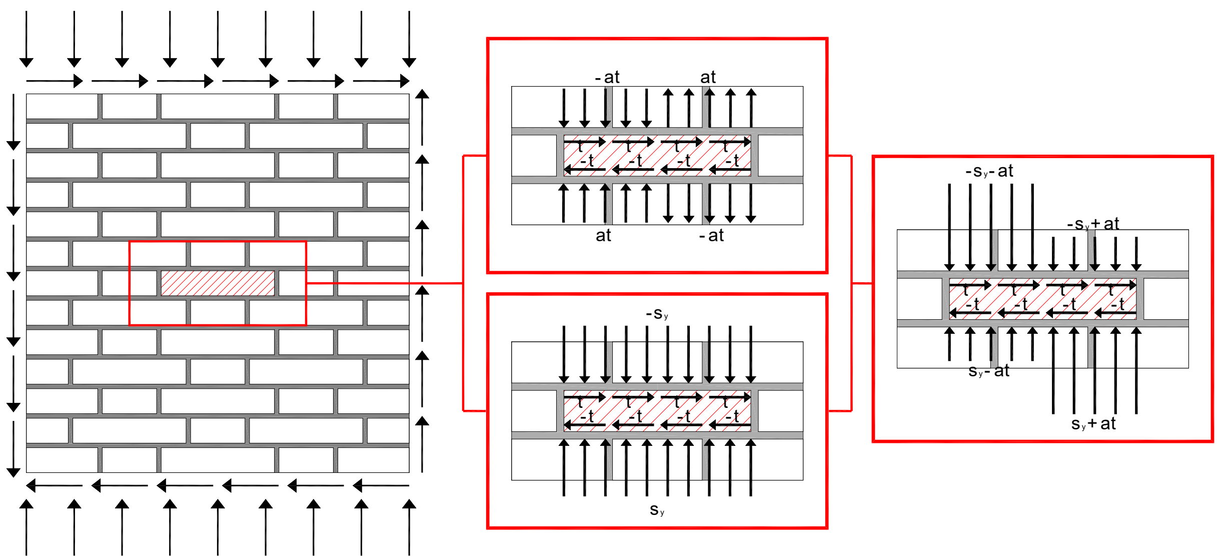

Figure 3: Non-uniform stress distribution at the brick near the panel's centroid due to compression/shear stresses.

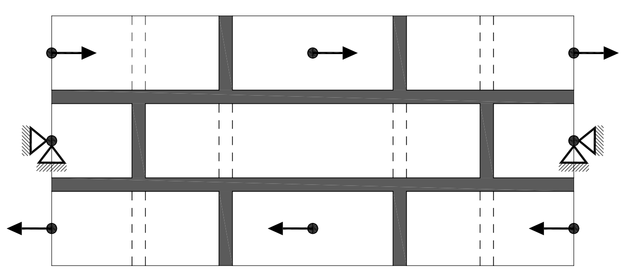

Figure 4: Boundary conditions and imposed horizontal displacements used to replicate the experimental conditions.

Horizontal displacements and boundary conditions (Figure 4) were therefore imposed to take into account for such antisymmetric deformation mechanism, which can lead to differentiated failures or material degradation at the bed and head joints.

3.2. Model assumptions

As both the initial and induced non-isotropy strictly depend on the geometrical arrangement of the units and the mortar, in the proposed approach the discontinuous nature of masonry was investigated through the use of a damage mechanic approach for each of the constituents at the detailed micro-scale (brick units and mortar joints), which were both modelled as a continuum with an isotropic multi-linear compressive stress-strain curve (i.e. linear strain hardening followed by a residual plateau of ideally plastic behavior). In opposition to the cohesive surface approach [30] [31], this allowed to take into account the real dimensions of masonry components as well as the Poisson's effect in the mortar joints, giving a better description of damage evolution from bed to head joints.

In such a context, damage simulation in the cuboid sub-cells was accomplished by the use of the Willam and Warnke (WW) [34] model along with a maximum tensile stress (tension cut-off) failure criterion. Such a smeared cracked model, originally adopted for concrete and other brittle materials, is able to account for both cracking and crushing failure modes, ensuring at the same time convexity (i.e. monotonically curved surface without inflection points) and smoothness (i.e. no sharp edges) of the yield function f(σ) defined as:

$$f(\sigma) = f(\sigma_a, \tau_a, \eta) = \frac{1}{r(\sigma_a, \eta)} \frac{\tau_a}{f_{cWW}} - 1 \geq 0 \tag{1}$$

where f_{cWW} represent the uniaxial compressive strength; σ_a and τ_a are the average normal and shear stress components defined in terms of principal stresses ($\sigma_1 \langle \sigma_2 \langle \sigma_3$) by proper expressions into four different domains (i.e. TTT, TTC, TCC and CCC; with T = tension and C = compression):

$$\sigma_a = \frac{1}{3}(\sigma_1 + \sigma_2 + \sigma_3) \qquad \tau_a = \begin{cases} \sigma_i \quad i = 1,2,3 & \text{TTT domain} \\ \sigma_i \quad i = 1,2 & \text{TTC domain} \\ \frac{1}{\sqrt{15}}\left[(\sigma_2 - \sigma_3)^2 + \sigma_2^2 + \sigma_3^2\right] & \text{TCC domain} \\ \frac{1}{\sqrt{15}}\left[(\sigma_1 - \sigma_2)^2 + (\sigma_2 - \sigma_3)^2 + (\sigma_3 - \sigma_1)^2\right] & \text{CCC domain} \end{cases} \tag{2}$$

and r(σ_a; η) is the mathematical expression for the deviatoric cross section (consisting of three tangent ellipses) of a conical failure surface defined as:

$$r(\sigma_a,\eta)=\frac{\sqrt{2r_2\left(r_2^2-r_1^2\right)\cos\eta+r_2(2r_1-r_2)\left[4\left(r_2^2-r_1^2\right)\cos^2\eta+5r_1^2-4r_1r_2\right]}}{4\left(r_2^2-r_1^2\right)\cos^2\eta+(r_2-2r_1)^2} \tag{3}$$

with:

$$\cos\eta=\frac{2\sigma_1-\sigma_2-\sigma_3}{\sqrt{2\left[\left(\sigma_1-\sigma_2\right)^2+\left(\sigma_2-\sigma_3\right)^2+\left(\sigma_3-\sigma_1\right)^2\right]}} \tag{4}$$

where η (anomaly or angle of similarity) and r_1, r_2 (position vectors or meridians) denote the polar coordinates of the representative point of the stress state in the deviatoric plane.

Assuming that, as in most practical cases [35], the hydrostatic stress is limited by f_{cWW}, the adopted failure surface was specified by using only two (instead of five) material parameters[1]: uniaxial compressive (f_{cWW}) and tensile (f_{tWW}) strength (assigned in agreement with the material properties obtained experimentally, see Section 4).

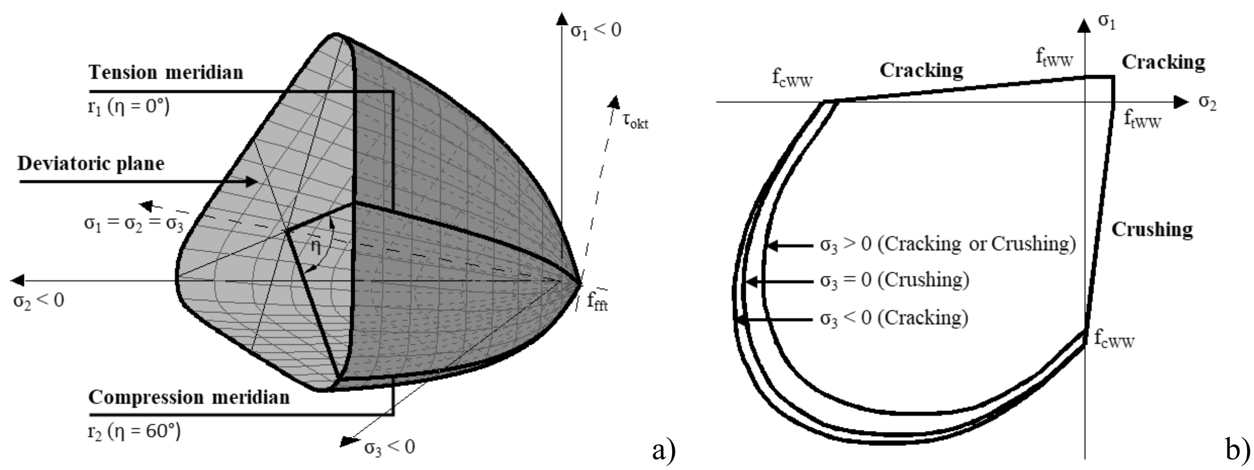

Figure 5: WW failure surface in principal stress space: a) Multiaxial stress case ($|\sigma_1|>|\sigma_2|>|\sigma_3|>0$); b) Nearly biaxial stress case ($|\sigma_1|>|\sigma_2|>0 \wedge |\sigma_3|\cong 0$).

Figure 5 illustrates a graphical representation of the WW failure surface. The shape of the three-dimensional interface in the space of principal stress (Multiaxial stress case, Figure 5a) consists of a conical failure surface with: two smooth convex meridians, approximated by two II-order parabolas along η = 0° (tension meridian, r_1) and η = 60° (compression meridian, r_2) with a common apex (corresponding to hydrostatic tension $f_{tt} = \sigma_a/f_{cWW}$) on the equisectrix ($\sigma_1 = \sigma_2 = \sigma_3$), and the deviatoric curve $r(\sigma_a;\, \eta)$, used as based section to interpolate the position vector (r) between the

[1] As for shear behavior, the model also permitted the introduction of two transfer coefficients (β_c and β_t), that account for a strength reduction of the shear stress causing sliding across the crack face for re-closed (β_c) or open cracks (β_t).

compression and tension meridians. Furthermore, the in-plane failure envelope of the periodic basic cell subjected to a macroscopically homogeneous shear state (Figure 4) was illustrated. It is noteworthy to point out how multiaxial stress case includes, in fact, biaxial or nearly biaxial stress case ($|\sigma_1|>|\sigma_2|>0 \wedge |\sigma_3|\cong 0$) as a special case [36], leading to three failure surfaces shown as projections of the three-dimensional failure surface in the σ_1-σ_2 plane. As shown in Figure 5b, although the three closed curves are nearly equivalent and continuous, the mode of failure is therefore a function of the sign of σ_3.

According to this approach, prior to failure, the response is elastic, whereas once the failure criteria for crushing was satisfied, the stiffness of the corresponding element was reduced to a negligible value. On the other hand, in case of cracking, a tension cut-off failure criterion was used and the stress-strain relations were modified by introducing a plane of weakness in a direction perpendicular to the crack face. Thus, for the direction in which cracking occurs, tensile strength essentially becomes zero, whereas material property for the directions in which crack has not occurred remains the same. A noteworthy point is that, as for the simulation of the contacts between masonry component, the unit-mortar interfaces were assumed to be perfect and their failure was thus not explicitly considered. Nevertheless, their overall effect was however incorporated modifying the mortar strength (fracture energy and mode I strength) such that they represent the tensile bond strength.

Lastly, as for the reinforcement, among the different modelling strategies proposed in literature (discrete or smeared representation), it was decided to adopt a discrete element method [37][38]. The reinforcing system was thus supposed to represent a volume of cement mortar (or epoxy paste) inside an extended composite continuum. More specifically, assuming a perfect bond (i.e. no slip was considered between mortar and rod truss elements), the reinforcing titanium rods surrounded by a cementitious (or epoxy) matrix were modelled as cementitious (or epoxy) beams (elastic solid elements with isotropic properties) with a reinforcing rod (tension-only truss elements) at the center of the beams (Figure 6). This gives a material law characterized by a linear-elastic behavior until a peak tensile stress is reached, after which the stress drops to zero immediately and the material fails in a brittle manner.

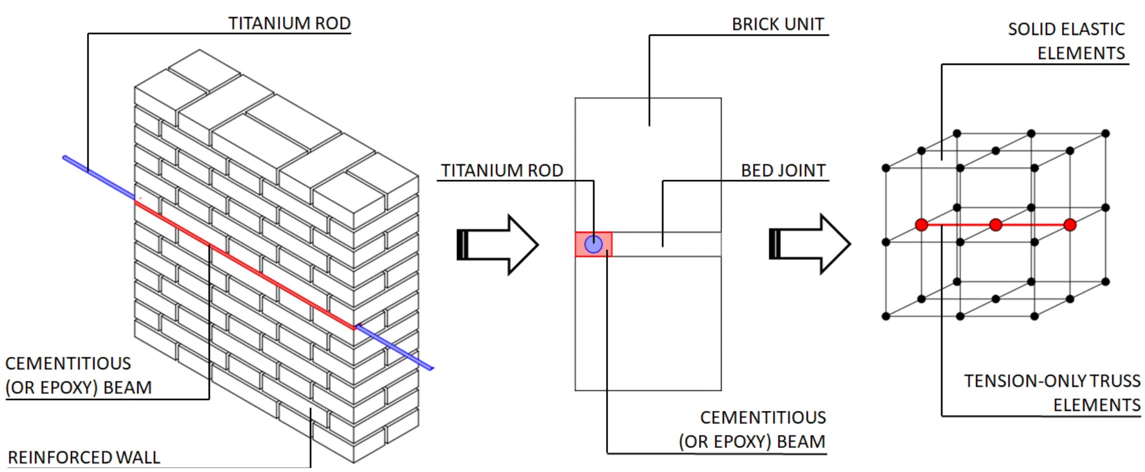

Figure 6: Discrete modelling of reinforced masonry

3.3. FE modelling

The micro-structure of both brick units and mortar was considered as an assemblage of densely packed isoparametric solid elements (Solid 65) of hexahedral shape (with eight nodes and three degrees of freedom at each node). A shared node approach was adopted for modelling the reinforcement rod inside cementitious (or epoxy) elements. To this end, the connection between the reinforcement and cementitious (or epoxy) matrix meshes was achieved treating the reinforcing rods (modelled using two-noded linear bar elements, Link 180) as a slave material that is merged to the surrounding master material.

For convergence checking, the periodically repeating arrangement of the basic cell was discretized with a sufficient number of elements across the sub-cells' heights. After performing sensitivity analyses using different mesh sizes, the FE mesh was in fact refined so as to have six elements (10×10×9 mm^3) across each brick unit, four elements (10×10×2.5 mm^3) across each bed or head joint (it is worth noticing how in the micro-modelling the mesh size was dictated by the mortar joints thickness) and three elements (10×10×2.5 mm^3) across the cementitious (or epoxy) matrix. This guarantees the more critical details to be captured without distorted meshes and, consequently, localization and shear lock effects. Figure 7 illustrates the full FEM: it consists of 38,220 elements and 41,870 nodes, with 125,610 degrees of freedom (DOF).

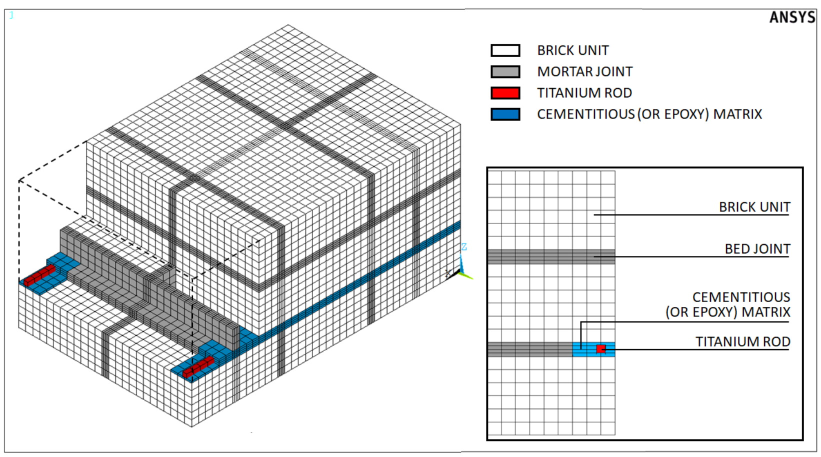

Figure 7: FE model with mesh discretization.

3.4. FE analysis

To investigate the reinforcement action of titanium rods, embedded into the mortar bed joints, a set of numerical analyses was carried out, varying the type of matrix (cementitious or epoxy). To this end, the numerical models were firstly subjected to their self-weight and an uniformly distributed load (σ_z = 0.2 MPa), followed by a horizontal displacement (displacement-controlled shear tests) under different displacement stages (minimum = 20, maximum = 40 steps).

Figure 8 to Figure 10 show the cracking pattern at increasing values of shear deformation (γ) for each analysis. As for the unreinforced specimen (Figure 8), cracking initiated at the half part of the bed joints under tensile stress (Figure 8a) and spread along the whole mortar plane. By increasing the shear strain, the mortar head joints partially failed, while the bed joints were fully cracked

(Figure 8b). This failure mode was mainly governed by the low mechanical properties of the mortar, producing early cracking of the horizontal joints and anticipating brick failures.

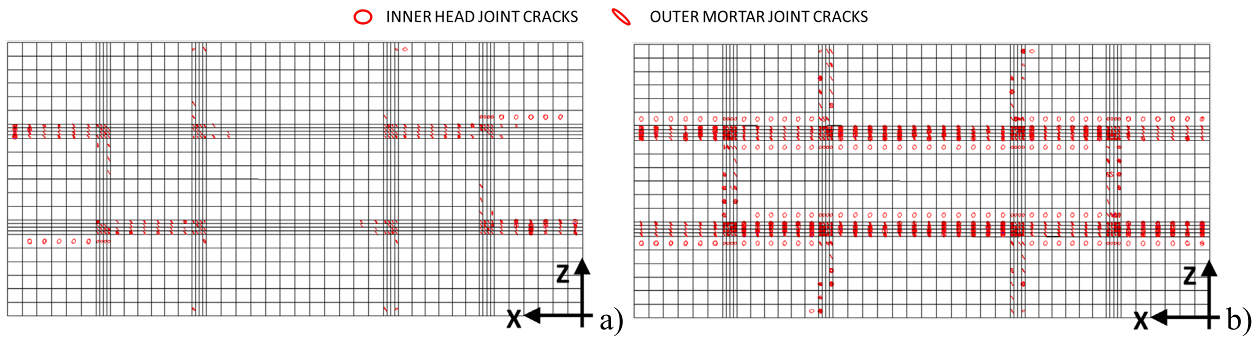

Figure 8: Cracking pattern of the unreinforced FE model (the red circles at each element centroid have their plane aligned with the cracking plane): a) at initial state of damage ($\gamma = 0.28\times10^{-4}$); b) at the end of analysis ($\gamma = 0.77\times10^{-4}$).

As expected, the positive effect of the reinforcing rods led to an expansion of the post-breaking phase, even if with a different damage evolution. Because of the reinforcement, for both types of matrix, the tensile damage firstly involved the head joints (Figure 9a and Figure 10a) and only for a high shear strain, propagated into the bed ones (Figure 9b and Figure 10b). In this situation, although the head joints were diffusely damaged[2], the reinforced prisms were still able to withstand shear stresses. Regardless of the type of matrix (cementitious or epoxy), the load-carrying capacity of the reinforced masonry was conserved as long as the reinforcing system was effective in stitching the shear cracks. When the rods could not further fulfill this positive action the bearing capacity suddenly decreased and the prisms failed.

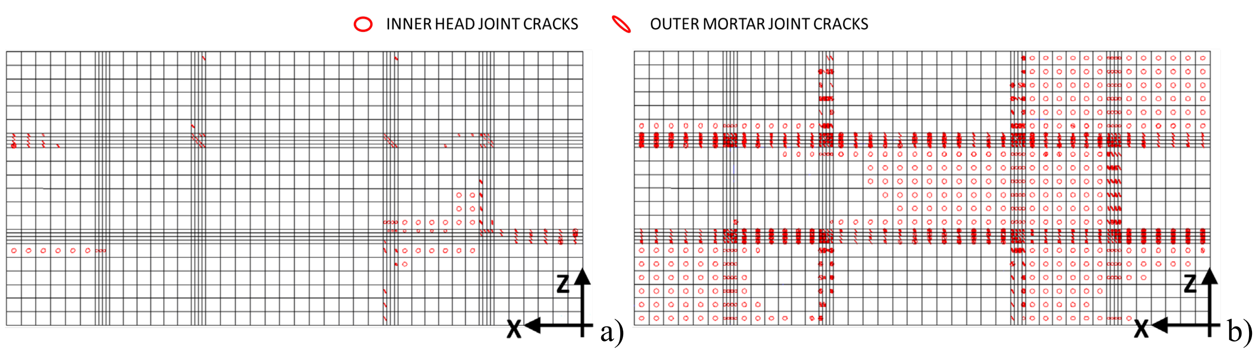

Figure 9: Cracking pattern of the reinforced (with cement mortar) FE model (the red circles at each element centroid have their plane aligned with the cracking plane): a) at initial state of damage ($\gamma = 0.28\times10^{-4}$); b) at the end of analysis ($\gamma = 0.77\times10^{-4}$).

---

[2] Compared with the crack pattern found in the case of titanium rods embedded in a cement mortar, in the case of epoxy paste a more widespread and diffused crack pattern was found.

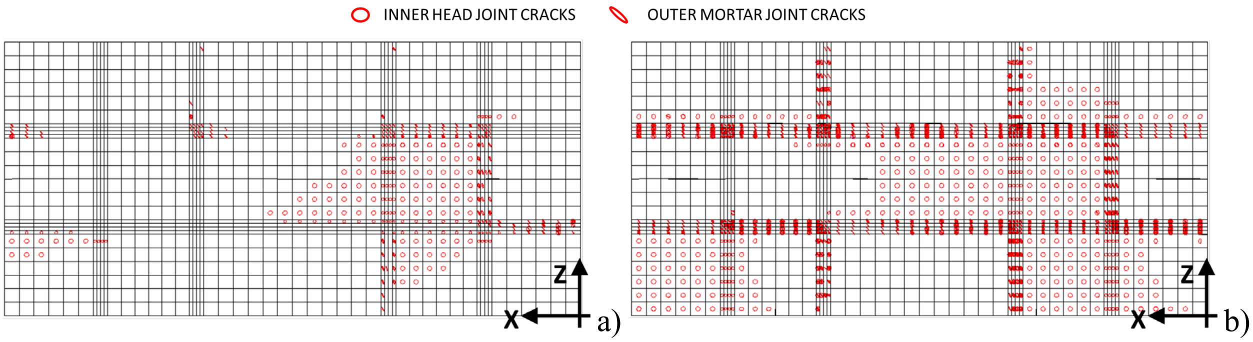

Figure 10: Cracking pattern of the reinforced (with epoxy paste) FE model (the red circles at each element centroid have their plane aligned with the cracking plane): a) at initial state of damage ($\gamma = 0.28\times10^{-4}$); b) at the end of analysis ($\gamma = 0.77\times10^{-4}$).

4. TEST ARRANGEMENT

A total of ten shear tests were carried out: an experimental testing program was implemented in the laboratory to investigate the diagonal tension strength of the brickwork masonry before and after the titanium repair. Two steel shoes were positioned at the panel's corners along a diagonal: these served to apply and distribute the diagonal shear load. A steel frame consisting of four steel rods was used for testing purposes: when loaded developed tension forces, consequently compressing the wall panel diagonally. The wall specimens were tested using a 500 kN single-acting hydraulic cylinder, diagonally positioned at a panel's corner between the contrast and a loading steel shoe. The shear test was conducted under load control at a rate of about 350 N/s up until failure was recorded. The diagonal compression load was gradually increased using a hydraulic manual pump. For shear deformation measurements, two LVDTs (Linear Variable Displacement Transducers) were used. The dimensions of the wall panels, the position of the diagonal load and LVDTs are shown in Figure 11.

All panels were identically repaired by twelve Ø7 mm titanium rods. Shear resistance is provided by two mechanisms, shear reinforcement (V_s) and the masonry (V_c). The equation used to estimate the shear capacity of masonry members in ASTM-E519 [39] standard is listed as Eq. (5). The standard testing procedure requires the rotation of the wall panel by 45° and vertical loading along one of the wall's diagonals. However, wall panels were tested in this test campaign avoiding this rotation.

$$S_S = 0.707 \frac{P_{\max}}{A_n} \qquad (5)$$

The masonry tensile strength can be calculated using:

$$f_t = 0.5 \frac{P_{\max}}{A_n} \qquad (6)$$

where P_{max} is the maximum diagonal force and A_n is the net area of the cross section wall panel, given by:

$$A_n = \left(\frac{w+h}{2}\right)t \qquad (7)$$

where t is the panel thickness (250 mm), w and h are the panel's width (900 mm) and the height (880 mm).

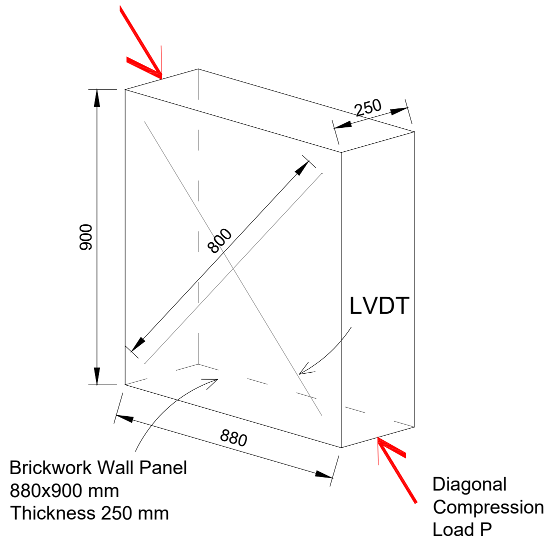

Figure 11: Details of the wall panel considered in the investigation.

It is also possible to compute the maximum shear strength τ_0 at the centroid of the wall panel. According to the RILEM formulation, this is given by:

$$\tau_0 = \frac{f_t}{1.5} \qquad (8)$$

With regard to the panel deformations under loading, the angular strain can be calculated using:

$$\gamma = |\varepsilon_c| + |\varepsilon_t| = \left(\frac{|\Delta V| + |\Delta H|}{L}\right) \qquad (9)$$

where ε_c and ε_t are the normal strains, and ΔV and ΔH are the shortening and stretching of the panel's diagonal in compression and tension, respectively, over a gage length (L) of 800 mm.

For the modulus of rigidity G, the following equation was used [40]:

$$G = \frac{\sigma_{xy}}{\gamma} = \frac{1.05(0.33P_{\max} - 0.03P_{\max})}{A_n(\gamma_{0.33P\max} - \gamma_{0.05P\max})} \qquad (10)$$

The deformations of wall panel were measured using two LVDTs mounted along the panel's diagonals. A pressure gage attached with a manual pump was used to measure the pressure and diagonal shear load. This load was applied in cycles with increasing amplitudes (increment of 10 kN per each cycle) up to failure (Figure 12).

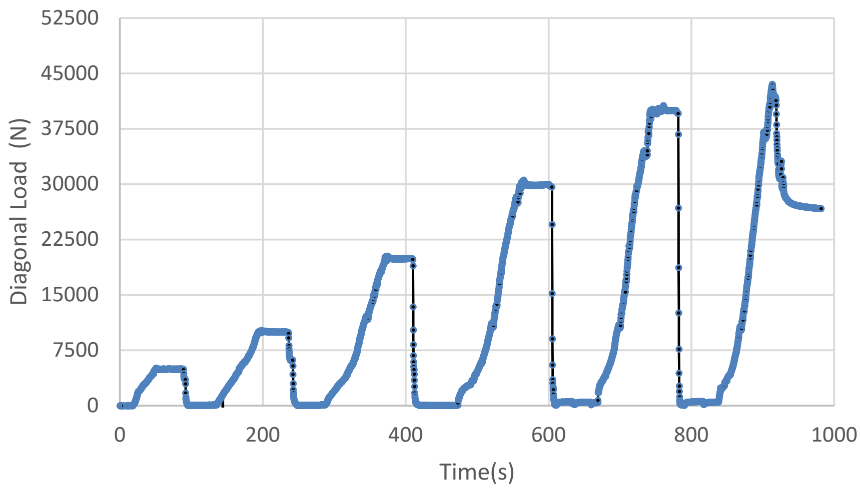

Figure 12: Typical diagonal load vs. time plot (BR-URM04).

5. MATERIALS PROPERTIES

The material properties of the masonry (bricks and mortar) and titanium were evaluated in the laboratory and are listed in Table 1 and Table 2.

5.1. Masonry

In order to simulate a real case scenario, wall panels were of one-brick thickness (250 mm). The brickwork was built in Flemish bond (this is made by laying stretchers and headers alternately in each course. Each stretcher is centered on the header of the course below). Used bricks were solid and made to a standard brick size of 250 mm long, 120 mm wide and 55 mm high. Nominal 10 mm mortar joints were used for construction.

Historic walls are typically made of mortars characterized by low mechanical properties. In central Italy the compressive strength of hand-made solid fired bricks and historic mortars are typically in the range of 20-45 and 4-8 MPa, respectively [41-43]. To simulate a historic wall, a low-cement mortar was employed for panel construction. Lime, sand and Portland cement were mixed in a volume ration of volume ratio of 1:2:0.15. An accurate gauging of mortar component materials was used to ensure the correct mortar designation and the desired constant performance. Fresh mortar was cast in three gang moulds for mortar prisms 40 x 40 x 160 mm made from steel conforms to EN 196 standard [44] specifications. Mortar prisms were initially tested in bending and subsequently in compression on the resulting halves. Test results show a bending strength of 0.22 MPa with a Coefficient of Variation (CoV) of 19.23% (Tab. 1). The compressive strength was 6.61

MPa (CoV 23.2%): this value is consistent with the typical mechanical characteristics of historic lime mortars [45-46].

On opposite, the bending and compressive strengths of the solid clay bricks were much higher (6.04 and 25.3 MPa, respectively). The compressive strength of brick was obtained in accordance with ASTM C67-11 [47] , by testing 12 bricks. These results are consistent with the mechanical properties of a historic mortar and hand-made solid bricks. Wall panels were assembled at the Structures Laboratory of the University of Perugia, Italy as per conventional site construction practice in Italy with the help of a local experienced mason.

Table 1: Measured material properties (*nominal dimensions).

	Mortar	Brick
Density (kg/m^3)	-	1613
Mix design (aerial lime: sand: cement)	1:2:0.15	-
Block dimensions (mm)	-	250x120x55*
Compressive Strength (MPa)	6.61	25.3
Young's modulus (MPa)	-	7565
Sample Size	6	10
CoV (%)	23.2	14.9
Bending Strength (MPa)	0.22	6.04
Sample Size	3	3
CoV (%)	19.3	16.1

5.2. Titanium solid rods

A commercially available 7 mm-diameter titanium rod was used in the current study (Figure 13). Rods are produced by Tifast, located in Narni, Italy [48]. The experimental program initially included characterisation of titanium rods [49] to determine their Yield and tensile strengths (Table 2).

Figure 13: The titanium rods used for repair.

Table 2. Measured mechanical properties of titanium rods used for repair (*0.2% offset strain method).

Number of tested samples	6
Alloy type	Ti-6l-4V
Nominal diameter (mm)	7
Weight density (kg/m^3)	4421
Yield Strength* / Standard Deviation (MPa)	977.5 / 118.3
Young's Modulus / Standard Deviation (GPa)	112.9 / 7.06
Tensile Strength / Standard Deviation (MPa)	1100.6 / 110.0

5.3. Materials used for rod application

Wall panels were repaired using titanium smooth rods embedded into a cement mortar or an epoxy paste. The results of the mechanical characterization of both the cement mortar [50] and the epoxy are reported in Table 3. The compressive strengths of the cement mortar and epoxy paste were 22.17 and 52.1 MPa, respectively, while the tensile/bending strengths are typically very low for a cement mortar and high for an epoxy.

Table 3: Mechanical properties of the bonding agents used for rod application (*nominal dimensions).

	Cement Mortar	Epoxy Paste
Mix design (lime: sand: cement)	1:2:1	-
Sample dimensions (mm)	160x40x40*	cylinder: 25
Compressive Strength / Standard Deviation	22.17 / 3.59	52.1 / 6.2
Young's modulus (GPa)	18.75	23.56
Sample Size	6	6
Bending Strength / Standard Deviation (MPa)	0.22 / 0.042	-
Sample Size	3	-

6. BOND LENGTH

To develop their tensile strength, reinforcement rods have to act together with masonry in resisting the external load. This depends on the mechanical properties and compatibility of the two materials (titanium and masonry). The reinforcing titanium rod has to undergo the same strain as the surrounding mortar or epoxy resin in order to prevent the separation of the two materials under loading.

The bond strength depends on several factors: the type of used cement mortar or resin, the tensile strength ratio of the materials, the mutual adhesion between the mortar/resin and titanium interfaces, the superficial treatment and shape of the titanium rod, the pressure of the hardened mortar/resin against the titanium rod due to the drying shrinkage of the mortar/resin and the level of the diagonal load during testing. Unfortunately, it was not possible to have a full control of these parameters: for example, smooth rods were used in this experiment when deformed rods would be expected to provide superior bond with the mortar or epoxy. However, deformed rods are not available in Italy on the construction market and the minimum rod diameter available is 7 mm. This is the consequence of the limited use of titanium, especially in the context of Civil engineering.

In order to prevent slippage phenomena, it was decided to use a high-strength cement mortar and a thixotropic (no-shrinkage) epoxy. Thirteen bond tests (pull-out tests) were carried out in the laboratory: titanium rods were inserted into a 25 mm-diamater steel tube, filled with mortar or resin. In this pull-out test, a titanium rod confined in a filled tube was pulled out and the pull-out load and the front displacement were recorded: although the confinement action activated by the steel tube is different from the one in the mortar joint, it is believed that test results are comparable with the expected behavior of the titanium bars inside the mortar joints. Figure 14 shows the results in terms of pull-out loads and bond length. It can be noted that the use of an epoxy guaranteed a high bond with small bond lengths. By using a bond length of 150 mm, it was possible to reach a maximum (average) shear stress of 2.94 MPa. This value is much higher than the shear strength of the masonry [51-52], making unnecessary to reach higher shear stresses at interface epoxy-rod. A bond length of 150 mm was selected for the subsequent shear tests on repaired wall panels.

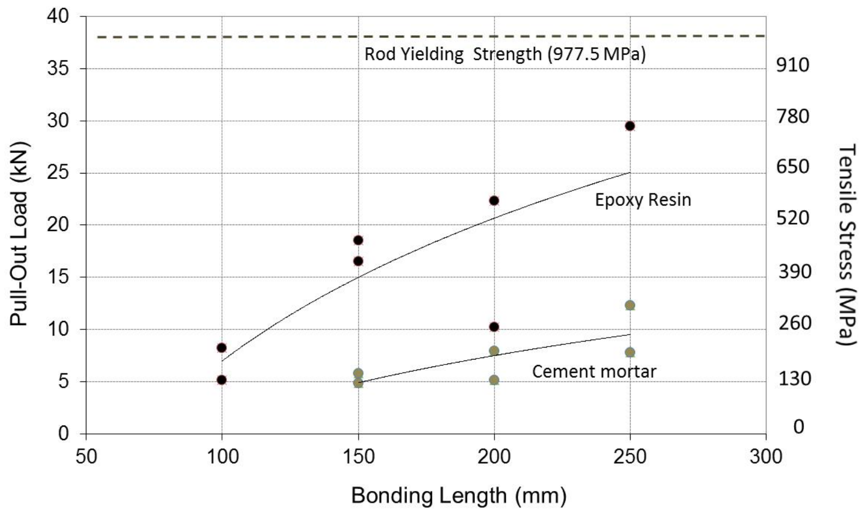

Figure 14: Bonding length vs. failure load/tensile stress for pull-out tests.

With regard to the use of the cement mortar, it was noted that lower pull-out loads and shear stresses were recorded. These values were about 67, 59, 65% smaller compared to corresponding tests using the same bond length (150, 200, 250 mm, respectively). Taking into consideration the typical shear strength of brickwork masonry [47], it was decided that a bond length of 175 mm (total rod length 350 mm) could be sufficient to repair a crack in a brickwork wall. A trend line of the pull-out load is also plotted for the tests carried out using the epoxy and cement mortar. The failure mode of all bond tests was due to the pull-out of the titanium rod from the metal cylinder. The cement mortar or the epoxy remained always fully attached to the metal cylinder.

7. SHEAR TEST RESULTS

Comprehensive test data were recorded in the experimental study, which comprised the diagonal crack propagation process, the panel's strains, and the deformation profiles at every load increment. It should be initially noted that we used a shear set-up avoiding the 45° rotation of the wall specimen: in this way, similarly to a real case-scenario of a wall panel subject to a seismic load, we expect some effect on the post-peak load behaviour. After failure, the gravity and shear loads acting along the diagonal, shear crack will generate phenomena of mechanical interlocking. This will provide a more "plastic" response of the wall panel after failure, with a some significant residual capacity.

Each test is identified by a 7-digit alpha-numeric code. The first two letters (BR) specify the construction material (solid tile bricks). The subsequent three-letter designation (URM for unreinforced control panels, RCE for panels repaired with titanium rods embedded into a cement mortar, and REP for panels repaired using an epoxy paste) was used to identify the repair method. Finally, a number was used to identify each panel.

A summary of ultimate load and maximum shear strain for each wall panel is presented in Table 4, together with the failure mode. The wall panels were initially tested in shear and used as control samples. These were loaded to ultimate failure. The wall panels were subsequently repaired with titanium rods and re-tested.

The control wall specimens acted, at least initially, as a single monolithic member. By increasing the diagonal load, shear strain linearly increased. In this situation, the standard elastic theory may be used to study the structure during the initial uncracked mode. The duration of the mode depends greatly on the mechanical properties of mortar used for wall construction. Since the mortar was weak, mortar cracking started occurring and the structural response of the wall panels tuned non-elastic and non-linear.

Table 4: Shear tests results.

Test No.	Max Diagonal Load $(P_d)_{max}$ (kN)	$(P_d)_{max,repaired}$ / $(P_d)_{max,URM}$	Shear Strength S_S (MPa)	Shear Strength τ_0 (MPa)	Angular Strain at 0.33 $(P_d)_{max}$ (%)	Shear Modulus $G_{1/3}$ (MPa)
BR-URM1	38.1	-	0.121	0.0571	0.01833	3271
BR-URM2	45.0	-	0.143	0.0674	0.02252	3151
BR-URM3	43.9	-	0.140	0.0658	0.01711	4041
BR-URM4	43.5	-	0.139	0.0652	0.01185	5750
(mean)	(42.6)	-	(0.135)	(0.0639)	(0.01695)	(4053)
BR-RCE1	22.1	0.518	0.070	0.0331	0.631	55.1
BR-RCE2	18.5	0.434	0.059	0.0277	0.430	68.5
(mean)	(20.3)	0.476	(0.065)	(0.0304)	(0.530)	(62)
BR-REP3	32.5	0.762	0.103	0.0487	0.241	212
BR-REP4	30.7	0.720	0.098	0.0460	0.434	111
(mean)	(31.6)	0.741	(0.100)	(0.0473)	(0.293)	(162)

Since shearing force predominated, the system acted as an in-plane loaded membrane and shear cracks developed along the diagonal in compression. This terminated the initial uncracked mode. Cracks followed a zig-zag pattern inside the mortar joints or at interface brick-to-mortar (Figure 15).

Figure 15: Typical diagonal cracking of control URM wall specimens.

For URM specimens, no-damage or very limited damage was observed in the bricks at the end of the test. After failure, the thickness of the shear cracks increased: the effect of mechanical interlocking along the shear crack progressively reduced: this caused a gradual loss of the panel's lateral capacity. At the end of the shear test, this varied between 30 and 50% of the maximum diagonal load.

Four repaired wall panels have been tested in this experiment. Titanium rods have been em-bedded into the cracked bed joints using a cement mortar (2 panels, test No. BR-RCE1 and BR-RCE2) or an epoxy paste (2 panels, test No. BR-REP3 and BR-REP4). The response of the repaired was found to be very different in terms of lateral capacity and shear modulus, depending on the type of material (cement mortar or epoxy paste) used for rod application.

The cement mortar was not able to guarantee a satisfactory stress-transfer, without slippage phenomena at interface rod-to-mortar. Few seconds after the application of the diagonal load, in correspondence of a very small values of the diagonal loads (4-5 kN), cracking occurred in the cement mortar used for repair. This was the result of the debonding (from both the bricks and the titanium rods) of the cement mortar used to fix the rods inside the horizontal mortar joints. The diagonal crack, previously opened when the URM panel was initially tested, re-opened for a mean diagonal load of 20.3 kN (corresponding to a shear strength τ_0 of 0.0304 MPa), 53.4% smaller compared to the shear strength of control specimens (Figure 16). It can be noted that this strength value is very similar to the residual load capacity of URM panels, after failure. This clearly demonstrates that the use of a cement mortar is not able to prevent the re-opening of the shear (diagonal) crack, compromising the repair action of the titanium rods.

Post-test survey revealed that cracking mainly occurred through mortar bed joints, with a very small number of cracks propagated through the brick units. The failure mode of repaired wall panels (using a cement mortar) was basically identical to the one recorded for URM panels.

A possible reason for this unsatisfactory structural response the fact that titanium rods were smooth. In order to overcome this problem, different solutions are under consideration at the moment: the use of longer titanium rods, ribbed rods in order to activate mechanical interlocking, the use of stronger cement mortars. Since the deboning was also recorded at brick-to-mortar interface, the use of ribbed rods could result non-effective.

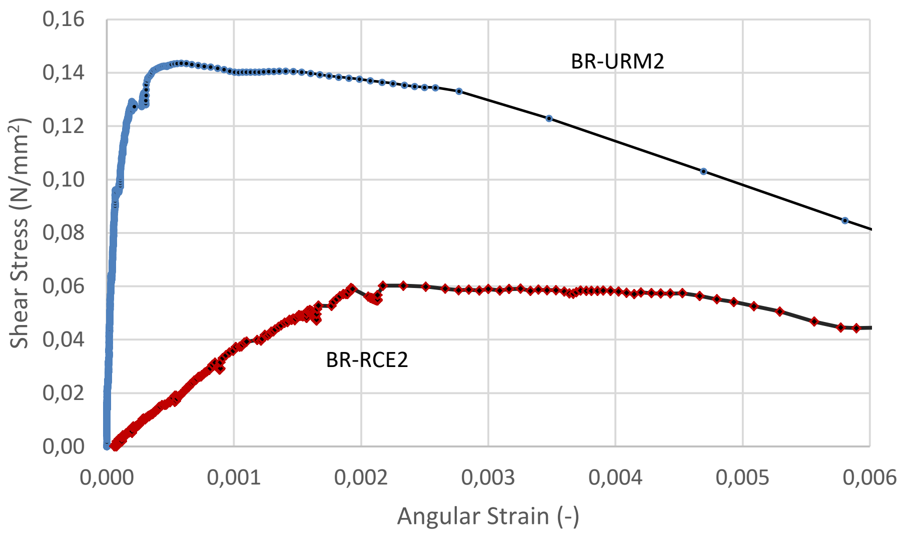

Figure 16: Angular strain vs. shear stress for tests No. BR-URM2 and BR-RCE2.

A similar unsatisfactory result can be noted in terms of shear modulus $G_{1/3}$ and corresponding angular strain: the high values of these mechanical parameters demonstrate again that the titanium rods did not contribute in the resisting action under panel's diagonal loading, due to poor stress transfer. At the end of the tests, an inspection of the titanium rods highlighted their complete detachment from the cement mortar with no damage.

The use of the epoxy paste to embed the rods into the horizontal mortar joints (Figure 17) produced improved test results. Figure 19 shows the shear stress – angular strain response, and load history of the repaired panel BR-REP4. This panel exhibited a linear response up to a shear stress S_S of approx. 0.08 MPa. The mean lateral capacity of the repaired wall panels was 31.6 kN, corresponding to a shear strength τ_0 of 0.0487 MPa, calculated using eq. (8). If we compare these results with the values recorded for URM panels (42.6 kN and 0.0639 MPa, respectively), it can be noted that the titanium rod repair was not able to restore the original lateral capacity of URM panels. However, the titanium rods were effective in stitching the crack: the combined action of the titanium rod and the epoxy resin prevented the re-opening of the crack in the original position and no slippage phenomena were recorded at interface brick-to-resin or resin-to-rod.

However, the panel's response in terms of shear deformations, although linear, was not likely elastic. Figure 18 shows that panel BR-REP4 highly deformed in shear (at maximum lateral load, angular strain was in the range 0.0030-0.0033 mm/mm). This large value of the angular strain clearly demonstrates that other phenomena of cracking occurred in the panel: it should be remarked here that the titanium rods were not effective in repairing the crack *inside* the panel. Furthermore, other small shear cracks started developing near the repaired area, with a progressive extension of their length.

Figure 17: A repaired wall panel using titanium rods for crack stitching.

In general, up to 76% of the original lateral capacity was exhibited by the epoxy-rod repaired panels. The failure mode of the repaired panels consisted in the formation of a new diagonal crack (along the diagonal in compression), outside the area where the rods have been previously installed. This crack only opened in the mortar joints, without affecting the bricks and the bed joint repaired with the titanium rod. Figure 19 is illuminating: it shows a detail of the diagonal crack at the end of the shear test. The epoxy is still perfectly bonded to the brickwork. Failure is due to cracking of the mortar used for panel construction, diagonal cracking outside the repaired zone and peeling phenomena of the bricks.

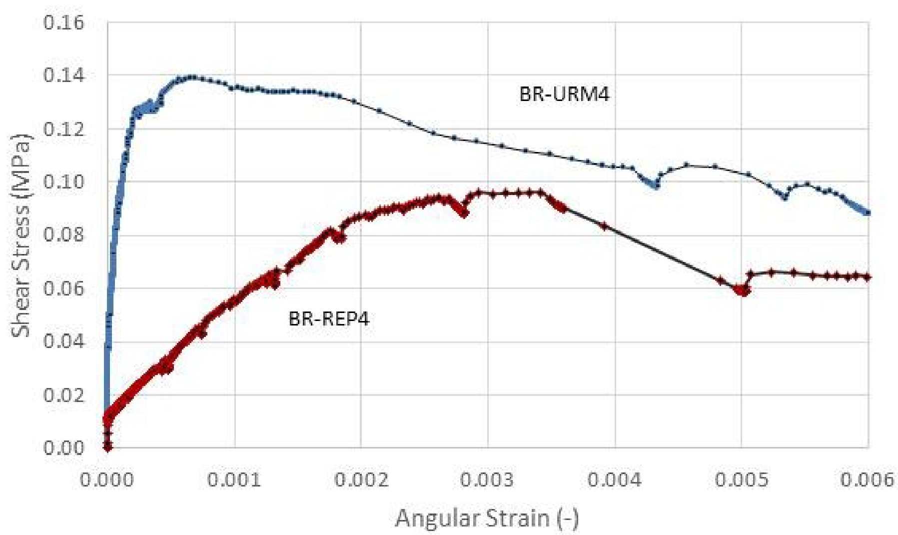

Figure 18: Angular strain vs. shear stress for tests No. BR-URM4 and BR-REP4.

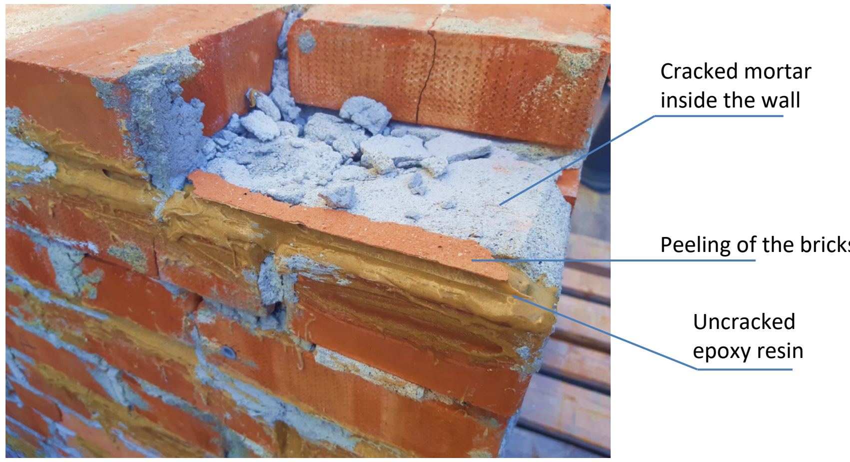

Figure 199: Detail of the diagonal crack of a repaired panel (with epoxy resin): it can be noted the perfect bonding between the epoxy and the brickwork, the internal cracked mortar, the peeling of the bricks at interface brick-mortar.

It could be interesting to comment on the reduced lateral capacity of the repaired panels, compared to URM panels (Figure 18): firstly, it should be remarked here that the titanium rods were only located along the superficial area of bed joints (on both panel's sides): the cracked vertical joints and the internal area of the cracked panels were not affected by the application of the rods. Furthermore, only every other bed joint was repaired with the rods: all this weakened the effectiveness of the repair method, and it provides an explanation for the missing ability to restore the original lateral capacity after repair. The basic idea was to study a non-invasive, localized, repair intervention: this was the rationale for the use of a inorganic matrix (cement mortar), and short titanium bars. However, tests results clearly demonstrated critical aspects and important limitations, and more experiments will be necessary. The use of titanium rods is certainly interesting: titanium is the most chemically stable metal in nature, with high mechanical properties and low density. Furthermore, titanium exhibits negligible mechanical degradation from ageing.

A bonded resistance strain gauge was applied on a titanium rod, before embedment into the horizontal joint and epoxy application. The strain gauge was bonded to the rod and protected from contact with the epoxy with a small piece of plastic tape. The instrumented rod was the one near the centroid of the panel surface (Figure 17). The strain gauge was applied at rod mid-point.

Figure 20 shows the strain vs. time plot. It can be noted that the maximum strain was 367 $\mu\varepsilon$, corresponding to a tensile stress of 41 MPa. Clearly, the resulting values of stress are far from the tensile strength values of both the epoxy and the titanium rod, highlighting that the failure is mainly governed by the masonry material, outside the region of the repaired joint. A strain gauge was also applied for a panel repaired with the cement mortar. However, the measured strain values were very small (about 45 $\mu\varepsilon$) and difficult to interpret. This seems to confirm that the use of a cement mortar coupled smooth titanium rods is inappropriate and non-effective.

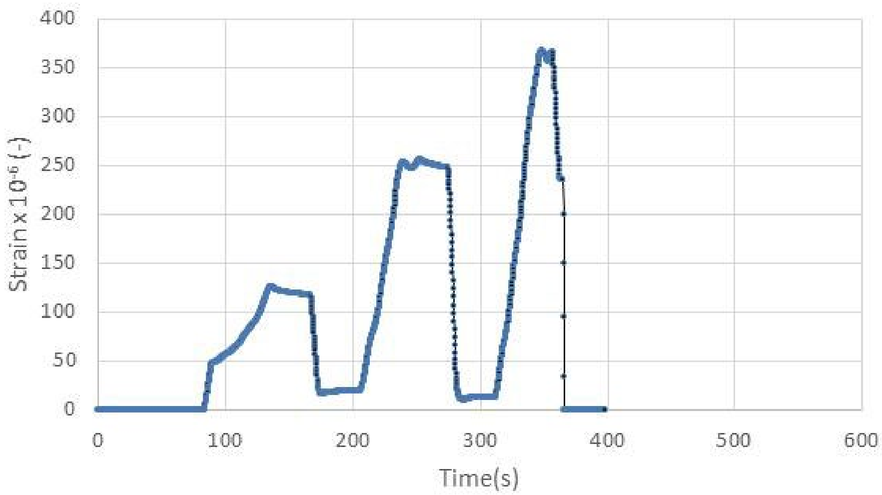

Figure 20: Tensile axial strains (strain gauge) of the titanium rod (at mid-point) vs. time (BR-REP4). After about 370 s from the beginning of the test, the gauge did not measure strains.

From the damage analysis at the end of the shear tests, it can be observed that no-cracking occurred in the area repaired with the titanium rods and the epoxy paste. Perfect rod-to-brick bonding across the crack was guaranteed by the epoxy. The failure mode of the URM walls was not limited by the formation of a single, diagonal crack: micro-cracking and a diffuse damage occurred inside the panel. The localized application of the titanium rod-repair wasn't able to repair the damage outside a limited panel's area. It is evident that the effective-ness of the repair depends on the level of damage of the URM panels: when this is localized (i.e. a single shear crack) the repairing method is more effective. On opposite, when the damage is made of a large number of cracks, it is more difficult to restore the original lateral capacity after rod repair.

It could be argued why the reinforced repointing wasn't extended to entire width of the walls. If titanium-to-masonry connection is effective, it should be initially noted that the repaired walls under the sharing, in-plane, force can basically fail only due to the development of a new shear (diagonal) crack outside the repaired area: this was an expected failure mode, however it was also expected that the corresponding lateral load capacity had to be consistent or greater than the capacity of the control, unreinforced walls, but this did not always occur. The aim of this experiment wasn't to reinforce or increase the wall capacity, but to repair the shear crack. This is the main reason because the reinforced-rod repointing wasn't applied in the area outside the cracks.

A similar comment could be made by looking at the shear moduli of both URM and re-paired wall panels. The use of high Young's modulus repair materials (23.56 and 112.9 GPa for the epoxy and the titanium rods, respectively) was not able to increase the panel's lateral stiffness, given the diffuse damage and crack pattern. The non-linear (un-elastic) response of URM wall panels after cracking highly reduced the lateral stiffness of the repaired panels, and the repair was not able to restore the original pre-damage stiffness. Again, the titanium rods ability to restore the original shear stiffness depends on the level and extension of the damage.

8. CONCLUSIONS

This paper reported the results of numerical and laboratory investigations of the structural behavior of brickwork wall panels repaired with smooth titanium rods embedded into the horizontal bed joints and subjected to in-plane shear loading. In detail, after checking the reinforcement action of titanium rods at local level through the use of a numerical procedure, laboratory tests were performed to investigate the effect of the proposed repair method at macro-scale level.

Based on the current study, the following conclusions can be drawn:

1. Unreinforced control specimen failed, as expected, due to the development of a inclined crack along the diagonal in compression. The crack had a zig-zag pattern and it only formed in the horizontal and vertical mortar joints;

2. The level of strength enhancement of titanium-repaired panels depends on the type of adhesive used for rod application (i.e. cement mortar or epoxy paste);

3. Premature debonding of the rods occurred in panels repaired with a cement mortar, which had lower strength compared to the panels repaired using an epoxy paste; shear strength of panels repaired with a cement mortar was only 47.6% of control specimens. For panels repaired with the epoxy paste, average shear strength was 74.1%; premature debonding of the installed titanium rods is a serious shortcoming of the proposed strengthening technique, and more tests will necessary to make the rod repair effective, for example avoiding the use of smooth rods or increasing the length and density of the titanium rods.

4. Both the use of a cement mortar and an epoxy paste was not sufficient to restore the original shear stiffness of control specimens: repaired panels exhibited a shear modulus up to 98% smaller compared to control specimens;

5. The experimental study on titanium repaired panels has shown that shear failures do not necessarily occur in the repaired area, and as such, the design of such members should be based on different criteria from those for wall panel strengthening. Walls panels repaired with titanium rods and epoxy resins failed due to the formation of a diagonal crack outside the repaired area of the panel.

In terms of reversibility of the intervention, it has to be preferred the use of an inorganic matrix (cement or hydraulic mortar) to bond the titanium rods to the masonry substrate. Unfortunately, this solution demonstrated to be ineffective. The use of an epoxy resin exhibits very limited characteristics of reversibility. Future research should concentrate on the use of reversible matrices, and, to improve bonding, ribbed or threaded titanium rods with longer bonding lengths.

9. ACKNOWLEDGEMENTS

The authors would like to acknowledge the Structures Laboratory, University of Perugia, Alessio Molinari and Emanuele Bombardieri. TiFast is acknowledged for its support of titanium rods. We also acknowledge the support from the the Italian Ministry for Research and Education, in funding this research, through the project "ReLUIS 2017-Linea murature" and ReLUIS SISMA 2016.

10. CONFLICT OF INTEREST

The authors declare that they have no conflict of interest.

11. REFERENCES

[1] Mastrodicasa S (1978) Dissesti statici delle strutture edilizie: diagnosi, consolidamento, istituzioni teoriche, Hoepli, Milan [in Italian]

[2] Binda L, Saisi A, Tiraboschi C (2000) Investigation procedures for the diagnosis of historic masonries, Constr Build Mat, 14: 199-233

[3] Borri A, Castori G, Corradi M (2012) Evaluation of shear strength of masonry panels through different experimental analyses. In: Proceeding of 14th Int. Conference Structural Faults, & Repair-2012, Edinburgh, Scotland

[4] Cardoso R, Lopes M, Bento R (2005) Seismic evaluation of old masonry buildings. Part I: Method description and application to a case-study. Eng Structures, 27: 2024-2035

[5] Cattari S, Degli Abbati S, Ferretti D, Lagomarsino S, Ottonelli D, Tralli A (2014) Damage assessment of fortresses after the 2012 Emilia earthquake (Italy). Bull Earth Eng, 12, 2333-2365

[6] Triantafillou TC (1998) Strengthening of masonry structures using epoxy-bonded FRP laminates. J Compos Constr, 2: 96-104

[7] Borri A, Corradi M, Vignoli A (2001) Seismic upgrading of masonry structures with FRP. In: Proceeding of 7th International Conference on inspection appraisal repairs and maintenance of buildings and structures, Nottingham, UK

[8] Capozucca R (2011) Experimental analysis of historic masonry walls reinforced by CFRP under in-plane cyclic loading. Compos Structures, 94 (1): 277-289

[9] Stratford T, Pascale G, Manfroni O, Bonfiglioli B (2004) Shear strengthening masonry panels with sheet glass-fiber reinforced polymer. J Compos Constr, 8(5): 434-443 (2004)

[10] ElGawady M, Lestuzzi P, Badoux M (2005) In-plane response of URM walls upgraded with FRP. J Compos Constr, 9(6): 524–535

[11] Tomazevic M, Weiss P, Velechovsky T, Apih V (1991) The strengthening of stone masonry walls with grouting. Structural repair and maintenance of historical buildings. Vol. 2: dynamics, stabilisation and restoration. Computational Mechanics Publications, Southampton, UK

[12] Vintzileou E, Tassios T (1995) Three-Leaf Stone Masonry Strengthened by Injecting Cement Grouts. J Struct Eng, 121(5): 848–856

[13] Baronio G, Binda L, Modena C (1992) Criteria and methods for the optional choice of grouts according to the characteristic of masonry, In: Proceeding of Int. Workshop

Effectiveness of Injection Techniques for Retrofitting of Stone and Brick Masonry Walls in Seismic Areas, CNR-GNDT, 139-157

[14] Corradi M, Borri A, Vignoli A (2008) Experimental evaluation of in-plane shear behavior of masonry walls retrofitted using conventional and innovative methods, Masonry International, 21(1): 29-42

[15] ICOMOS Charter, Principles for the analysis, conservation and structural restoration of architectural heritage. ICOMOS 14th General Assembly and Scientific Symposium, Victoria Falls, Zimbabwe

[16] Mack RC, Speweik JP (1998) Repointing mortar joints in historic masonry buildings, Preservation Briefs, 1-16

[17] Valluzzi MR, Binda L, Modena C (2005) Mechanical behavior of historic masonry structures strengthened by bed joints structural repointing, Constr Build Mat, 19(1): 63-73

[18] Maurenbrecher AHP, Trischuk K, Rousseau MZ, Subercaseaux (2008) Repointing mortars for older masonry buildings – site considerations, Construction Technology Update, 6

[19] Corradi M, Tedeschi C, Binda L, Borri A (2008) Experimental evaluation of shear and compression strength of masonry wall before and after reinforcement: deep repointing, Constr Build Mat, 22(4): 463-472

[20] Cecchi A, Barbieri A (2008) Homogenisation procedure to evaluate the effectiveness of masonry strengthening by CFRP repointing technique, WSEAS Transactions on Applied and Theoretical Mechanics, 3(1): 12-27

[21] Gams M, Tomaževič M, Kwiecieǹ A (2015) Strengthenig brick masonry by repointing – an experimental study, Key Engineering Materials, 624: 444-452

[22] Valluzzi MR, Binda L, Modena C (2005) Mechanical behaviour of historic masonry structures strengthened by bed joints structural repointing, Constr Build Mat, 19(1): 63-73

[23] Borri A, Corradi M, Speranzini E, Giannantoni A (2009) Reinforcement of historic masonry: the "Reticolatus" technique, In: Proceeding of 13th scientific-technical Conference - Remo 2009 Repair, Conservation and strengthening of traditionally erected buildings and historic buildings, Wroclaw, Poland

[24] Corradi M, Borri A, Castori G, Sisti R (2016) The Reticulatus method for shear strengthening of fair-faced masonry, B Earth Eng, 14(12): 3547-3571

[25] Ismail N, Petersen RB, Masia MJ, Ingham MJ Diagonal shear strength of unreinforced masonry wallettes retrofitted using twisted steel bars, Constr Build Mat, 25(12): 4386-93

[26] Helifix, www.helifix.co.uk, accessed 9 June 2019

[27] Corradi M, Borri A, Costanzi M, Monotti S (2019) In-plane behavior of cracked masonry walls repaired with titanium rods, In: Proceeding of 7th ECCOMAS Thematic Conference on Computational Methods in Structural Dynamics and Earthquake Engineering. Crete, Greece

[28] Gabor A, Ferrier E, Jacquelin E, Hamelin P (2006) Analysis and modelling of the in-plane shear behavior of hollow brick masonry panels, Constr Build Mater, 20(5): 308-321 (2006)

[29] Castori G, Borri A, De Maria A, Corradi M, Sisti R (2017) Seismic vulnerability assessment of a monumental masonry building, Eng Struct, 136, 454-465

[30] Lourenço PB, Rots JG, Blaauwendraad J (1995) Two approaches for the analysis of masonry structures: micro and macro-modeling, Heron, 40(4): 313-340

[31] Penava D, Sigmund V, Kožar I, Anić F, Trajber D, Vig M (2015) Spatial Micromodel of the Masonry Wall. In: Proceeding of 8th ICCSM 8th International Congress of Croatian Society of Mechanics, Opatija, Croatia.

[32] Addessi D, Marfia S, Sacco E, Toti J (2014) Modeling Approaches for Masonry Structures, Open Civ Eng J, 8: 288-300

[33] Mann W, Müller H (1980) Failure of shear-stressed masonry – an enlarged theory, tests and application to shear-walls, In: Proceedings of the international symposium on load bearing brickwork, London, UK

[34] Willam KJ, Warnke ED (1975) Constitutive model for the triaxial behaviour of concrete. In: Proceeding of the International Association for Bridge and Structural Engineering, Bergamo, Italy

[35] Torelli G, D'Ayala D, Betti M, Bartoli G (2020) Analytical and numerical seismic assessment of heritage masonry towers, Bull Earthquake Eng, 18: 969–1008

[36] Betti M, Galano L, Vignoli A (2016) Finite element modelling for seismic assessment of historic masonry buildings, Earthquakes and their impact on society. Earthquakes and Their Impact on Society. Springer, Berlin

[37] Sarhosis V, Lemos JV (2018) A detailed micro-modelling approach for the structural analysis of masonry assemblages, Comput Struct, 206: 66-81

[38] Sarhosis V, Forgács T, Lemos JV (2019) A discrete approach for modelling backfill material in masonry arch bridges, Comput Struct, 224: 106108

[39] ASTM E519 / E519M (2010) Standard Test Method for Diagonal Tension (Shear) in Masonry Assemblages

[40] Brignola A, Frumento S, Lagomarsino A (2008) Identification of shear parameters of masonry panels through the in-situ diagonal compression test, Int J Architect Herit, 3(1): 52-73

[41] Hand-made fired bricks, mechanical properties, kiln Bernasconi, Italy, data sheet available at https://www.fornacebernasconi.com/wp-content/uploads/2019/01/catalogo-bernasconi-MATTONI-PER-MURATURA-2018-web.pdf

[42] Binda L, Mirabella Roberti G, Tiraboschi C. (1996) Problemi di misura dei parametri meccanici della muratura e dei suoi componenti. Proc. Conf. La Meccanica delle Murature tra Teoria e Progetto, Messina, Italy.

[43] Fernandes F, Lourenço PB (2007) Evaluation of the compressive strength of ancient clay bricks using microdrilling. Journal of materials in civil engineering, 19(9): 791-800.

[44] EN 196-1, Methods of Testing Cement, Determination of Strength.

[45] Lanas J, Bernal JP, Bello MA, Galindo JA (2004) Mechanical properties of natural hydraulic lime-based mortars. Cement and concrete research, 34(12): 2191-2201.

[46] Moropoulou A, Bakolas A, Moundoulas P, Aggelakopoulou E, Anagnostopoulou S (2005) Strength development and lime reaction in mortars for repairing historic masonries. Cement and Concrete Composites, 27(2): 289-294.

[47] ASTM C67 (2011) Standard Test Methods for Sampling and Testing Brick and Structural Clay Tile

[48] Titanium Expo, TITANIUM USA 2018, Las Vegas, NV, USA

[49] STM B348, Standard Specification for Titanium and Titanium Alloy Bars and Billets, 2013

[50] Penava D, Radic I, Gazic G, Sigmund V (2011) Mechanical properties of masonry as required for the seismic resistance verification, Tehnicki Vjesnik, 18(2): 273-280

[51] Corradi M, Borri A. (2018) A database of the structural behavior of masonry in shear, Bull Earthquake Eng, (9): 3905-30

[52] Boschi S, Galano L, Vignoli A. (2019) Mechanical characterisation of Tuscany masonry typologies by in situ tests, Bull Earthquake Eng, 17(1): 413-38